AWARD NUMBER: W81XWH-13-1-0280

TITLE: Targeting Androgen Receptor by Lysosomal Degradation in Prostate Cancer

PRINCIPAL INVESTIGATOR: Yuzuru Shiio

CONTRACTING ORGANIZATION: University of Texas Health Science Center at San Antonio
San Antonio, TX 78229

REPORT DATE: September 2014

TYPE OF REPORT: annual

PREPARED FOR: U.S. Army Medical Research and Materiel Command
Fort Detrick, Maryland 21702-5012

# REPORT DOCUMENTATION PAGE

*Form Approved*
*OMB No. 0704-0188*



| 1. REPORT DATE | 2. REPORT TYPE | 3. DATES COVERED |
|---|---|---|
| September 2014 | Annual | 01Sep2013-31Aug2014 |

**4. TITLE AND SUBTITLE**

Targeting Androgen Receptor by Lysosomal Degradation in Prostate Cancer

**5a. CONTRACT NUMBER**

**5b. GRANT NUMBER**
W81XWH-13-1-0280

**5c. PROGRAM ELEMENT NUMBER**

**6. AUTHOR(S)**

Yuzuru Shiio

E-Mail: shiio@uthscsa.edu

**5d. PROJECT NUMBER**

**5e. TASK NUMBER**

**5f. WORK UNIT NUMBER**

**7. PERFORMING ORGANIZATION NAME(S) AND ADDRESS(ES)**

The University of Texas
Health Science Center at San Antonio
San Antonio, TX 78229

**8. PERFORMING ORGANIZATION REPORT NUMBER**

**9. SPONSORING / MONITORING AGENCY NAME(S) AND ADDRESS(ES)**

U.S. Army Medical Research and Materiel Command
Fort Detrick, Maryland 21702-5012

**10. SPONSOR/MONITOR'S ACRONYM(S)**

**11. SPONSOR/MONITOR'S REPORT NUMBER(S)**

**12. DISTRIBUTION / AVAILABILITY STATEMENT**

Approved for Public Release; Distribution Unlimited

**13. SUPPLEMENTARY NOTES**

**14. ABSTRACT**

Androgen receptor (AR) plays a critical role in the progression of prostate cancer. This project is directed towards testing the feasibility of targeting AR for lysosomal degradation. We have demonstrated that AR can indeed be targeted for degradation by stimulating the TFEB – lysosome degradation pathway either by increasing the TFEB levels or by activating TFEB using mTORC1 kinase inhibitor, torin 1. Additionally, we determined that the same approach can be used to target the EWS-Fli-1 oncoprotein for degradation.

**15. SUBJECT TERMS**
Androgen receptor, lysosome, degradation, prostate cancer, TFEB, torin 1

| 16. SECURITY CLASSIFICATION OF: | | | 17. LIMITATION OF ABSTRACT | 18. NUMBER OF PAGES | 19a. NAME OF RESPONSIBLE PERSON |
|---|---|---|---|---|---|
| a. REPORT | b. ABSTRACT | c. THIS PAGE | | | USAMRMC |
| Unclassified | Unclassified | Unclassified | Unclassified | 18 | 19b. TELEPHONE NUMBER *(include area code)* |

**Standard Form 298 (Rev. 8-98)**
**Prescribed by ANSI Std. Z39.18**

## Table of Contents

**Page**

## 1. INTRODUCTION

Androgen receptor (AR) plays a critical role in the progression of prostate cancer. Prostate cancer is initially dependent on the ligand of AR, androgen, and androgen deprivation therapy is effective. However, over time, most patients develop androgen-independent disease, which no longer responds to hormonal therapies. Importantly, even at this advanced stage of androgen-independent disease, most tumors are still dependent on continued expression and activation of AR. Therefore, targeting AR is a promising approach to treat advanced prostate cancer. This project is directed towards testing the feasibility of targeting AR for lysosomal degradation. While most cellular proteins turn over by ubiquitin-proteasome-dependent mechanism, steroid hormone receptors including AR were recently shown to be substrates of lysosomal degradation (*1*). Although AR is also known to be degraded by ubiquitin-proteasome-dependent mechanism (*2*), the cellular pool of AR could be depleted by enhancing its lysosomal degradation. An important untested hypothesis, which will be tested in this project, is whether enhanced lysosomal degradation of AR can be used to target AR. To increase the lysosomal degradation, we will use either exogenous TFEB expression or a pharmacological activator of the TFEB – lysosome degradation pathway, torin 1, and test their effects on AR degradation.

## 2. KEYWORDS

androgen receptor, degradation, lysosome, prostate cancer, TFEB, torin 1, therapy

## 3. OVERALL PROJECT SUMMARY

In mid-2009, a transcription factor, TFEB, was shown to function as a master regulator of lysosomal biogenesis (*3*). The activity of TFEB is controlled by cytoplasmic sequestration, which is regulated by mTOR-mediated phosphorylation (*4-6*). A potent mTOR active-site inhibitor, torin 1, was shown to efficiently induce the nuclear translocation of TFEB (*4-6*). In contrast, rapamycin, an mTOR allosteric inhibitor that only incompletely inhibits mTOR activity, did not induce TFEB nuclear translocation at any of the concentrations that are routinely used (10 nM – 10 μM) (*4, 5*). Therefore, by overexpressing TFEB or by inducing TFEB nuclear translocation using torin 1, lysosomal biogenesis can be induced, which could be employed to degrade AR in prostate cancer.

In order to test the effect of TFEB on AR degradation, we generated the expression vectors for TFEB. We obtained a cDNA for human full-length TFEB, added a FLAG-tag at the N-terminus of TFEB using PCR, verified the DNA sequence of PCR-amplified cDNA, and cloned the tagged TFEB cDNA to pcDNA3 and pCDF1 expression vectors. We packaged the pCDF1-FLAG-TFEB lentivirus by co-transfection in 293T cells with pFIV-34N and pVSV-G packaging plasmids and generated the lentivirus expressing FLAG-TFEB. Robust expression of TFEB was verified by anti-FLAG immunoblotting of cell lysates prepared from cells infected with pCDF1-FLAG-TFEB lentivirus as well as cells transfected with pcDNA3-FLAG-TFEB expression vector. Additionally, anti-TFEB

immunoblotting demonstrated 5~10-fold increased levels of TFEB expression in cells infected with pCDF1-FLAG-TFEB lentivirus and in cells transfected with pcDNA3-FLAG-TFEB expression vector, compared with control cells expressing endogenous levels of TFEB. As mentioned above, the subcellular location of endogenous TFEB is regulated by mTOR-mediated phosphorylation. We therefore mutated the mTOR phosphorylation site in TFEB (S211A) to test whether TFEB S211A mutant displays more nuclear localization and hence would be more effective in inducing lysosomal biogenesis. Under the conditions of lentiviral expression or transient transfection, we did not observe increased nuclear localization of TFEB S211A compared with wild-type TFEB (both were mainly nuclear), suggesting that when exogenously expressed, a sufficient amount of wild-type TFEB localizes in the nucleus to induce the gene expression program for lysosomal biogenesis (*3*).

Using GFP-tagged AR expression vector, we were able to show that TFEB induces the degradation of GFP-AR (Figure 1A). The endogenous TFEB activity is regulated by mTOR-dependent phosphorylation (*4-6*). Phosphorylation by mTOR results in sequestration of TFEB in the cytoplasm and inhibition of lysosomal biogenesis. The activity of mTOR is negatively regulated by the TSC1/TSC2 tumor suppressor complex. A hypoxia-inducible protein, REDD1, was shown to inhibit the mTOR activity through TSC1/TSC2 (*7*). Consistent with this, co-expression of REDD1 resulted in reduced GFP-AR protein levels (Figure 1A).

**Figure 1 Targeting AR for degradation by the TFEB - lysosome pathway.**

**A**. Effect of TFEB, LAMP2, HSPA8, and REDD1 on the GFP-AR protein levels in 293 cells.
**B**. Effect of 100 μM chloroquine (CQ) or 300 nM torin 1 on the GFP-AR levels in 293 cells.

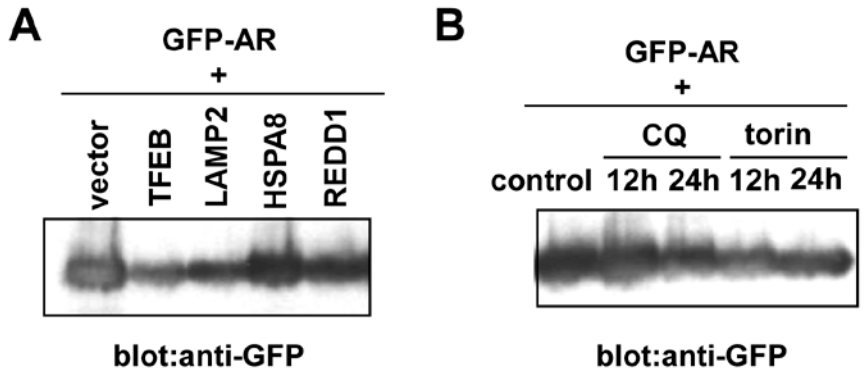


We have also analyzed the effect of LAMP2 and HSPA8, two key components of chaperone-mediated autophagy (CMA) on the AR protein levels, to assess the role of CMA in the lysosomal degradation of AR. Co-expression of LAMP2, which serves as a receptor and lysosomal import cargo for CMA substrates, significantly reduced GFP-AR expression (Figure 1A). LAMP2 co-expression was also shown to reduce the protein levels of HIF-1α, a recently proposed CMA substrate (*8*). Additionally, co-expression of HSPA8 also slightly reduced GFP-AR protein levels (Figure 1A) as was the case for HIF-1α (*8*). These results suggest a possible involvement of chaperone-mediated

autophagy in the lysosomal degradation of AR. While the link between the TFEB – lysosome pathway and chaperone-mediated autophagy is not yet established, chaperone-mediated autophagy might explain how AR is transported to the lysosome for degradation when the TFEB – lysosome pathway is activated.

As mentioned earlier, a kinase inhibitor of mTORC1, torin 1, potently inhibits the mTORC1 activity, leading to increased nuclear translocation of endogenous TFEB. We found that torin 1 reduced the protein levels of GFP-AR (Figure 1B). This is consistent with that inhibition of mTORC1 activity and activation of TFEB by torin 1 causes the degradation of AR.

GFP-AR was located in the nucleus and cytoplasmic dot-like structures. GFP-AR was also located in the nucleus and cytoplasmic dot-like structures upon TFEB co-expression or torin 1 treatment, suggesting that activation of the TFEB – lysosome pathway results in AR degradation without altering the subcellular location of AR.

These results support our central hypothesis that AR can be targeted for degradation by stimulating its lysosomal degradation via the TFEB – lysosome biogenesis pathway.

We encountered a technical difficulty with the detection of endogenous AR by immunoblotting and have now identified the anti-AR antibody (D6F11, Cell Signaling Technology) as an appropriate antibody for detection of endogenous AR. Using the reagents described above, we plan to complete the assessment of the effect of TFEB and torin 1 on AR protein levels and transcriptional activity in prostate cancer cell lines.

Additionally, we have used the same reagents developed by the course of this project to demonstrate the role of the TFEB – lysosome pathway in the turnover of EWS-Fli-1, a fusion oncoprotein of Ewing sarcoma (Note the research expenses for this experiment were paid by the institutional pilot grant, not by the present Department of Defense grant, but we acknowledged the support by this Department of Defense grant in our publication (*9*)).

We demonstrated that EWS-Fli-1 can be efficiently targeted for degradation by TFEB (Figure 2A) and a lysosomal protease, cathepsin D, can proteolyze EWS-Fli-1 both in 293 cells (Figure 2B) and in A673 Ewing sarcoma cells (Figure 2C). We went on to demonstrate that torin 1 treatment results in degradation of endogenous EWS-Fli-1 in A673 and TC71 Ewing sarcoma cells (Figure 2D), suggesting a novel therapeutic approach to target EWS-Fli-1 for degradation by stimulating the TFEB – lysosome degradation pathway. The paper describing this finding was published in the *Journal of Proteome Research* (*9*) and we have acknowledged the support by this Department of Defense grant award because we used the reagents developed by the latter grant project. (The research cost of the EWS-Fli-1 experiment was paid by an institutional pilot grant, not by this Department of Defense grant.) The findings on EWS-Fli-1 illustrate the translational direction to which we intend to develop the project on targeting AR for lysosomal degradation.

**Figure 2 Targeting EWS-Fli-1 for degradation by the TFEB - lysosome pathway.**

**A**. TFEB induces EWS-Fli-1 degradation in 293 cells.
**B**. Cathepsin D degrades EWS-Fli-1, but not p53, in 293 cells.
**C**. Cathepsin D degrades endogenous EWS-Fli-1 in A673 Ewing sarcoma cells.
**D**. Targeting endogenous EWS-Fli-1 for degradation by torin 1.

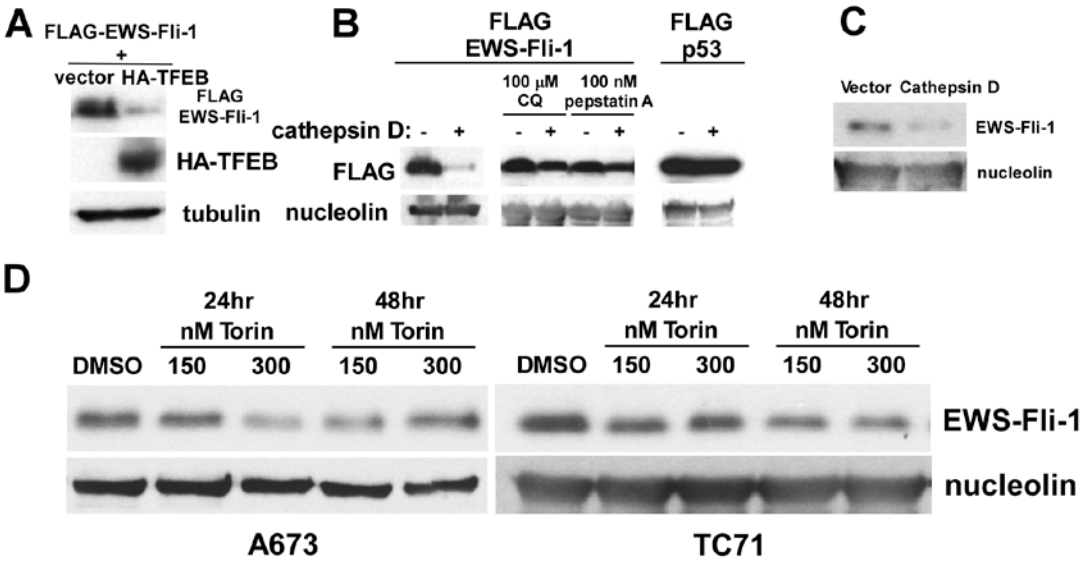


## 4. KEY RESEARCH ACCOMPLISHMENTS

- Demonstration of the feasibility of targeting AR for degradation by stimulation of the TFEB – lysosome pathway.
- Demonstration of the feasibility of targeting EWS-Fli-1 for degradation by the TFEB – lysosome pathway in Ewing sarcoma cells.

## 5. CONCLUSION

The completed portion of the project demonstrated the feasibility of targeting AR for degradation by activating the TFEB – lysosomal biogenesis pathway either by increasing the TFEB expression levels or by stimulating the TFEB activity by treatment with an mTORC1 kinase inhibitor, torin 1. We have now identified an appropriate reagent for detection of endogenous AR by immunoblotting and plan to complete the evaluation of the effect of TFEB and torin 1 on endogenous AR in prostate cancer cell lines. Using the reagents developed by the completed portion of the project, we also demonstrated that EWS-Fli-1 can be efficiently targeted for degradation by activating the TFEB - lysosome pathway, which has important therapeutic implications. The success with EWS-Fli-1 serves as a proof of principle of the selective targeting of cancer proteins for degradation.

6. PUBLICATIONS, ABSTRACTS, AND PRESENTATIONS

Publication in peer-reviewed scientific journals (which acknowledged the support by this grant award):

Elzi, D.J., Song, M., Hakala, K., Weintraub, S.T., and Shiio, Y.* (2014)
Proteomic analysis of the EWS-Fli-1 interactome reveals the role of the lysosome in EWS-Fli-1 turnover. *Journal of Proteome Research*, 2014 Jul 14. [Epub ahead of print].
*Corresponding author

A copy of this peer-reviewed publication is attached in the Appendix.

7. INVENTIONS, PATENTS AND LICENSES

Nothing to report.

8. REPORTABLE OUTCOMES

Peer-reviewed journal article publication:

Elzi, D.J., Song, M., Hakala, K., Weintraub, S.T., and Shiio, Y.* (2014)
Proteomic analysis of the EWS-Fli-1 interactome reveals the role of the lysosome in EWS-Fli-1 turnover. *Journal of Proteome Research*, 2014 Jul 14. [Epub ahead of print].
*Corresponding author

9. OTHER ACHIEVEMENTS

Nothing to report.

10. REFERENCES

1. Y. He *et al.*, Identification of a lysosomal pathway that modulates glucocorticoid signaling and the inflammatory response. *Sci Signal* **4**, ra44 (2011).
2. H. K. Lin, L. Wang, Y. C. Hu, S. Altuwaijri, C. Chang, Phosphorylation-dependent ubiquitylation and degradation of androgen receptor by Akt require Mdm2 E3 ligase. *Embo J* **21**, 4037 (Aug 1, 2002).
3. M. Sardiello *et al.*, A gene network regulating lysosomal biogenesis and function. *Science* **325**, 473 (Jul 24, 2009).
4. C. Settembre *et al.*, A lysosome-to-nucleus signalling mechanism senses and regulates the lysosome via mTOR and TFEB. *Embo J* **31**, 1095 (Mar 7, 2012).
5. A. Roczniak-Ferguson *et al.*, The transcription factor TFEB links mTORC1 signaling to transcriptional control of lysosome homeostasis. *Sci Signal* **5**, ra42 (Jun 12, 2012).
6. J. A. Martina, Y. Chen, M. Gucek, R. Puertollano, MTORC1 functions as a transcriptional regulator of autophagy by preventing nuclear transport of TFEB. *Autophagy* **8**, 903 (Jun, 2012).

7. J. Brugarolas *et al.*, Regulation of mTOR function in response to hypoxia by REDD1 and the TSC1/TSC2 tumor suppressor complex. *Genes Dev* **18**, 2893 (Dec 1, 2004).
8. M. E. Hubbi *et al.*, Chaperone-mediated autophagy targets hypoxia-inducible factor-1alpha (HIF-1alpha) for lysosomal degradation. *J Biol Chem* **288**, 10703 (Apr 12, 2013).
9. D. J. Elzi, M. Song, K. Hakala, S. T. Weintraub, Y. Shiio, Proteomic Analysis of the EWS-Fli-1 Interactome Reveals the Role of the Lysosome in EWS-Fli-1 Turnover. *J Proteome Res*, July 14 [Epub ahead of print] (Jul 14 2014).

11. Appendix

A copy of a peer-reviewed publication that acknowledged the support by this grant award is attached in the Appendix.

Journal of proteome research

Article

pubs.acs.org/jpr

Open Access on 07/07/2015

# Proteomic Analysis of the EWS-Fli-1 Interactome Reveals the Role of the Lysosome in EWS-Fli-1 Turnover

David J. Elzi,[†] Meihua Song,[†] Kevin Hakala,[‡] Susan T. Weintraub,[‡] and Yuzuru Shiio*[,†,‡]

[†]Greehey Children's Cancer Research Institute and [‡]Department of Biochemistry, The University of Texas Health Science Center, San Antonio, Texas 78229-3900, United States

Supporting Information

**ABSTRACT:** Ewing sarcoma is a cancer of bone and soft tissue in children that is characterized by a chromosomal translocation involving EWS and an Ets family transcription factor, most commonly Fli-1. EWS-Fli-1 fusion accounts for 85% of cases. The growth and survival of Ewing sarcoma cells are critically dependent on EWS-Fli-1. A large body of evidence has established that EWS-Fli-1 functions as a DNA-binding transcription factor that regulates the expression of a number of genes important for cell proliferation and transformation. However, little is known about the biochemical properties of the EWS-Fli-1 protein. We undertook a series of proteomic analyses to dissect the EWS-Fli-1 interactome. Employing a proximity-dependent biotinylation technique, BioID, we identified cation-independent mannose 6-phosphate receptor (CIMPR) as a protein located in the vicinity of EWS-Fli-1 within a cell. CIMPR is a cargo that mediates the delivery of lysosomal hydrolases from the trans-Golgi network to the endosome, which are subsequently transferred to the lysosomes. Further molecular cell biological analyses uncovered a role for lysosomes in the turnover of the EWS-Fli-1 protein. We demonstrate that an mTORC1 active-site inhibitor, torin 1, which stimulates the TFEB-lysosome pathway, can induce the degradation of EWS-Fli-1, suggesting a potential therapeutic approach to target EWS-Fli-1 for degradation.

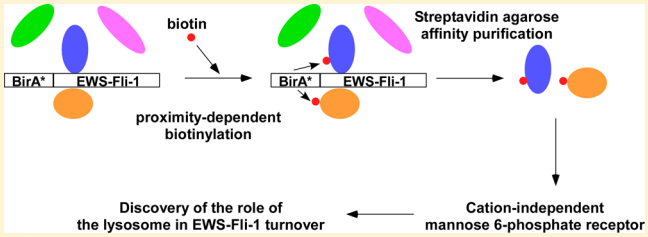


**KEYWORDS:** *EWS-Fli-1, Ewing sarcoma, interactome, proximity-dependent biotinylation, lysosome, protein degradation*

## INTRODUCTION

Ewing sarcoma is the second most common malignancy of bone and soft tissues in children and young adults and is characterized by a chromosomal translocation that generates a fusion oncogene between EWS and an Ets family transcription factor, most commonly Fli-1.[1−5] EWS-Fli-1 fusion accounts for 85% of Ewing sarcoma cases. Ewing sarcoma is an aggressive tumor with relatively poor long-term outcome. Overall survival is approximately 60%, and the five-year survival of recurrent cases is less than 10%. Considering that current cytotoxic chemotherapies used for Ewing sarcoma are not improving the survival of metastatic or recurrent disease, a new approach for targeted therapy needs to be developed.[1−5] The growth and survival of Ewing sarcoma cells critically depend on the EWS-Fli-1 fusion oncoprotein.[1−6] Therefore, targeting EWS-Fli-1 is a promising approach to treat Ewing sarcoma. However, despite a number of attempts, an EWS-Fli-1-targeted therapy has not materialized to date and EWS-Fli-1 continues to be "the perfect target without a therapeutic agent".[7]

EWS-Fli-1 is a transcription factor that controls the expression of a number of genes important for cell proliferation and transformation.[1−4] Transcriptional regulation by EWS-Fli-1 has been studied extensively, but little is known about the biochemical properties of the EWS-Fli-1 protein. To gain insight into the biochemical nature of the EWS-Fli-1 protein, we undertook proteomic analyses of the EWS-Fli-1 interactome. The result from the interactome analyses was used to provide leads for subsequent molecular biological analyses. Using a tandem affinity purification approach, we identified known EWS-Fli-1 interactors such as EWS[8] and RNA helicase A.[9] Using a proximity-dependent biotinylation technique, BioID,[10] we identified cation-independent mannose 6-phosphate receptor (CIMPR) as a protein located in the vicinity of EWS-Fli-1 within a cell. CIMPR is a cargo that mediates the sorting of lysosomal hydrolase precursors from the trans-Golgi network to endosomes.[11] Additional molecular cell biological analyses revealed that the EWS-Fli-1 protein turns over by a lysosome-dependent mechanism. We show that torin 1, which is an active-site inhibitor of mTORC1 that was shown to stimulate the TFEB-lysosome pathway, can reduce EWS-Fli-1 protein levels in Ewing sarcoma cells, suggesting a potential utility of mTORC1 active-site inhibitors as therapy for Ewing sarcoma.

## EXPERIMENTAL PROCEDURES

### Reagents

Chloroquine and pepstatin A were purchased from MP Biomedicals. Doxorubicin was purchased from Sigma-Aldrich.

**Received:** April 20, 2014
**Published:** July 7, 2014





dx.doi.org/10.1021/pr500387m | J. Proteome Res. 2014, 13, 3783−3791

Rapamycin and MG-132 were purchased from Calbiochem/EMD Biosciences. Cytosine arabinoside was from Tocris Bioscience. Torin 1 was from Cayman Chemical. The target sequences for shRNAs are as follows: human CIMPR shRNA, CTACCTGTATGAGATCCAA; human VPS26A shRNA, CTCTATTAAGATGGAAGTG; luciferase shRNA, GCACTCTGATTGACAAATACGATTT. Cathepsin D and firefly luciferase−EWS-Fli-1 fusion cDNAs were cloned into pCDF1 lentiviral vector (System Biosciences).

## Cell Culture

293 cells and 293T cells were cultured in Dulbecco's modified Eagle's medium (DMEM) supplemented with 10% calf serum. A673 cells and HeLa cells were cultured in DMEM supplemented with 10% fetal calf serum. TC71 cells were cultured in RPMI1640 medium supplemented with 10% fetal calf serum. Calcium phosphate coprecipitation was used for transfection of 293 and 293T cells. Lentiviruses were prepared by transfection in 293T cells following System Biosciences' protocol, and the cells infected with lentiviruses were selected with 2 μg/mL puromycin for 48 h as described.[12,13] Luciferase assays were done as described.[13]

## Protein Sample Preparation and Mass Spectrometry

**Tandem Affinity Purification of FLAG-His-EWS-Fli-1-Interacting Proteins.** Forty 15-cm plates of 293T cells were transfected with FLAG-His-EWS-Fli-1 (type 1 fusion); 48 h after transfection, the cells were lysed in TN buffer (10 mM Tris pH 7.4/150 mM NaCl/1% NP-40/1 mM AEBSF/10 μg/mL aprotinin/10 μg/mL Leupeptin/1 μg/mL Pepstatin A/20 mM sodium fluoride). The lysate was incubated with Ni-NTA agarose (Qiagen), FLAG-His-EWS-Fli-1 and its interacting proteins were collected by centrifugation, washed three times with TN buffer, and eluted with 50 mM sodium phosphate buffer pH 8.0/150 mM NaCl/250 mM imidazole. The eluted sample was immunoprecipitated with anti-FLAG antibody (M2, Sigma-Aldrich), the immunoprecipitate was eluted with FLAG peptide (Sigma-Aldrich), and the eluted protein sample was processed with an Amicon Ultra 0.5 3k centrifugal filter device (Millipore) for concentration and buffer exchange to 50 mM Tris pH 8.5. Proteins were digested at 37 °C overnight with trypsin (Promega; 1:10, enzyme/substrate) in the presence of 10% acetonitrile (ACN). The pH of the digestion solution was adjusted to 7.5 with 1 mM ammonium bicarbonate, if necessary. The resulting tryptic peptides were analyzed by HPLC-ESI-tandem mass spectrometry (HPLC-ESI-MS/MS) on a Thermo Fisher LTQ Orbitrap Velos mass spectrometer fitted with a New Objective Digital PicoView 550 NanoESI source. Online HPLC separation of the digests was accomplished with an Eksigent/AB Sciex NanoLC-Ultra 2-D HPLC system: column, PicoFrit (New Objective; 75 μm i.d.) packed to 15-cm with C18 adsorbent (Vydac; 218MSB5 5 μm, 300 Å); mobile phase A, 0.5% acetic acid (HAc)/0.005% trifluoroacetic acid (TFA); mobile phase B, 90% ACN/0.5% HAc/0.005% TFA; gradient 2−42% B in 120 min; flow rate, 0.4 μL/min. Precursor ions were acquired in the Orbitrap in centroid mode at 60,000 resolution ($m/z$ 400); data-dependent collision-induced dissociation (CID) spectra of the 10 most intense ions in the precursor scan above a threshold of 3,000 were acquired at the same time in the linear trap (isolation window for MS/MS, 3; relative collision energy, 30). Ions with a 1+ or unassigned charge state were not fragmented. Dynamic exclusion settings were: repeat count, 1; repeat duration, 30 s; exclusion list size, 500; exclusion duration, 30 s.

**BioID Proximity-Dependent Biotinylation Proteomics.** Three 15-cm plates of 293 cells were transfected with BioID-EWS-Fli-1 (Myc tag and BirA R118G mutant fused to the N-terminus of EWS-Fli-1). Twenty-four hours after transfection, biotinylation of proteins in the vicinity of BioID-EWS-Fli-1 within the cells was induced for 24 h by the addition of 50 μM biotin to the culture medium. The cells were lysed by boiling in a lysis buffer (50 mM Tris, pH 7.4/500 mM NaCl/0.4% SDS/5 mM EDTA/1 mM DTT/1 mM AEBSF/10 μg/mL aprotinin/10 μg/mL Leupeptin/1 μg/mL Pepstatin A/20 mM sodium fluoride). The viscosity of the sample was reduced by passing it through an 18-gauge needle followed by sonication. Triton X-100 was added to 2% final concentration, and the biotinylated proteins were purified using streptavidin agarose (Pierce/Thermo Fisher) and eluted in an SDS-PAGE sample buffer. The proteins in each sample were fractionated by SDS-PAGE and visualized by Coomassie blue. Each gel lane was divided into six slices, and the proteins in each slice were digested *in situ* with trypsin (Promega modified) in 40 mM $NH_4HCO_3$ overnight at 37 °C. The resulting tryptic peptides were analyzed by HPLC-ESI-MS/MS as described above, except that a 30 min HPLC gradient was employed and the six most intense ions in the precursor scan were fragmented.

## Mass Spectrometry Data Analysis

The Xcalibur raw files were converted to mzXML format using ReAdW (http://tools.proteomecenter.org/wiki/index.php?title=Software:ReAdW) and were searched against the IPI human protein database (v 3.24; 66,923 protein entries) using X! Tandem. Methionine oxidation was considered as a variable modification in all searches, and lysine biotinylation was included for the BioID experiments. Up to one missed tryptic cleavage was allowed. The X! Tandem search results were analyzed by the Trans-Proteomic Pipeline[14] version 4.3. Peptide/protein identifications were validated by Peptide/ProteinProphet.[15,16] A ProteinProphet score of 0.9 was used as a cutoff, which corresponded to false identification rates of 1.1% and 0.7% in the FLAG-His-EWS-Fli-1 and BioID-EWS-Fli-1 data sets, respectively.

## Immunoblotting

Immunoblotting was performed as described.[12,13] The following antibodies were used: rabbit polyclonal anti-CIMPR (ab32815, Abcam); mouse monoclonal anti-cyclin D1 (2926, Cell Signaling Technologies); mouse monoclonal anti-FLAG (M2, Sigma-Aldrich); rabbit polyclonal anti-FLAG (Immunology Consultants Laboratory, Inc.); rabbit polyclonal anti-Fli-1 (ab15289, Abcam); mouse monoclonal anti-HA (16B12, Covance); mouse monoclonal anti-LAMP2 (55803, BD Biosciences); rabbit polyclonal anti-mSin3A (K-20, Santa Cruz Biotechnology); rabbit polyclonal anti-Myc (N262, Santa Cruz Biotechnology); mouse monoclonal anti-nucleolin (C23, Santa Cruz Biotechnology); mouse monoclonal anti-p62/SQSTM1 (610832, BD Biosciences); and mouse monoclonal anti-tubulin (DM1A, Lab Vision).

## Preparation of the Lysosomes

A673 cells were treated with 100 μM chloroquine for 12 h or left untreated. Lysosomes were prepared using the Lysosome Enrichment Kit for Tissue and Cultured Cells (#89839, Pierce/Thermo Scientific) following the manufacturer's protocol. Briefly, cells were lysed by sonication in the manufacturer's lysis buffer and centrifuged at 500g for 10 min. The resulting supernatant was placed on top of a density gradient comprising

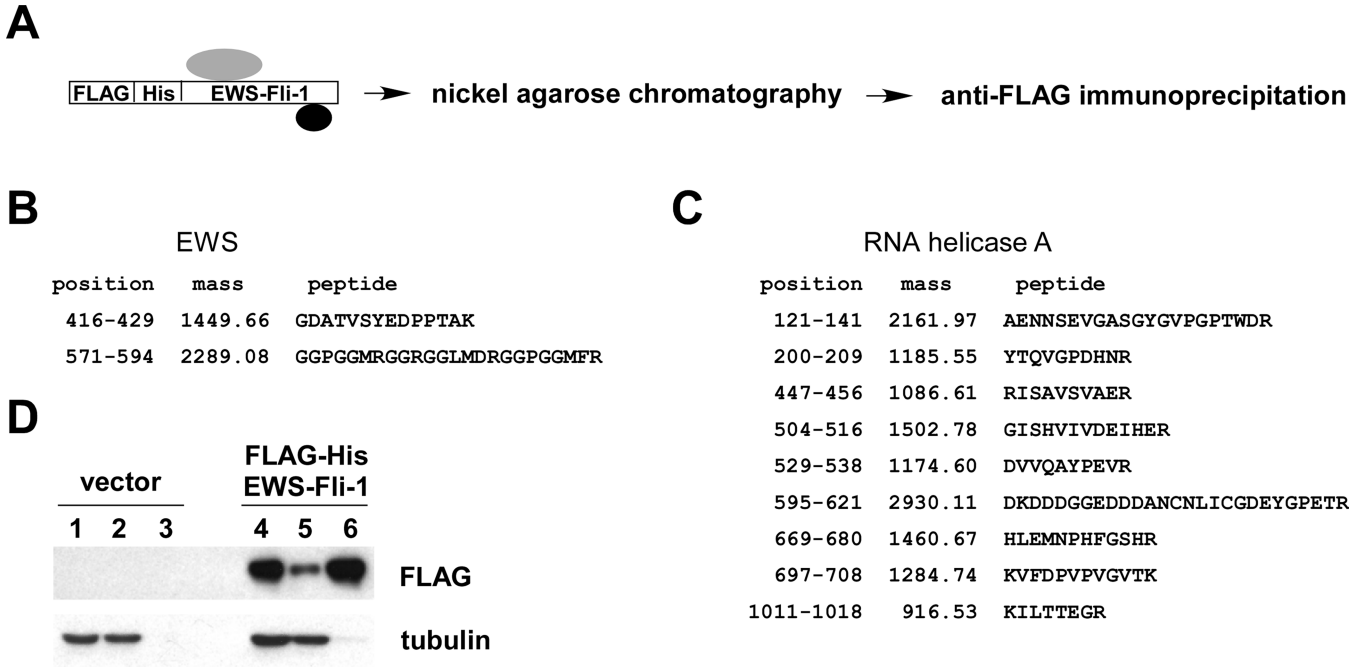


**Figure 1.** Tandem affinity purification analysis of the EWS-Fli-1-interacting proteins. (A) Tandem affinity purification procedure. 293T cells were transfected with FLAG-His-EWS-Fli-1. Forty-eight hours after transfection, FLAG-His-EWS-Fli-1 and its interacting proteins were isolated by nickel affinity chromatography followed by anti-FLAG immunoprecipitation and the protein sample was analyzed by tandem mass spectrometry. (B) EWS peptides assigned with high confidence. (C) RNA helicase A peptides assigned with high confidence. (D) FLAG-His-EWS-Fli-1 is mostly insoluble under the lysis conditions used for tandem affinity purification. The abundance of FLAG-His-EWS-Fli-1 in whole cell lysate (lane 1 and 4), tandem affinity purification lysate (lane 2 and 5), and postlysis pellet (lane 3 and 6) was determined by anti-FLAG immunoblotting. Tubulin serves as a loading control.

of 17% - 30% iodixanol -5,5′-[(2-hydroxy-1,3-propanediyl)-bis(acetylamino)] bis [*N*,*N*′-bis(2,3 dihydroxypropyl-2,4,6-triiodo-1,3-benzenecarboxamide)] in the manufacture's gradient dilution buffer, with an aliquot of the supernatant saved as the input fraction. The lysosome enrichment gradient was centrifuged at 145,000*g* using a SW60Ti rotor (Beckman-Coulter) for 2 h at 4 °C. The top layer of the gradient, which contains the lysosomes, was collected, diluted with two volumes phosphate-buffered saline, and centrifuged at 16,000*g* for 30 min at 4 °C. The resulting lysosome pellet was washed once in gradient dilution buffer and dissolved in SDS-PAGE sample buffer. For immunoblotting analysis, the lysosome fraction was loaded at 100x compared to the input.

## RESULTS AND DISCUSSION

### Proteomic Analysis of the EWS-Fli-1-Interacting Proteins

To dissect the EWS-Fli-1 interactome, we initially employed a tandem affinity purification approach. We expressed FLAG-His-tagged EWS-Fli-1 in human embryonic kidney 293T cells and isolated the EWS-Fli-1-containing protein complex by nickel agarose chromatography followed by anti-FLAG immunoprecipitation, which was subsequently analyzed by HPLC-ESI-MS/MS as described in the Experimental Procedures (Figure 1A). At a Protein Prophet probability score of 0.9 or higher, 105 different proteins were identified (Table S1). To exclude the false positive identifications, we employed the data sets obtained using two unrelated nuclear proteins, p21 (CDKN1A) and histone macroH2A. The proteins commonly identified by FLAG-His-EWS-Fli-1 and FLAG-His-p21 or FLAG-His-macroH2A with a Protein Prophet probability score of 0.9 or higher were considered as false positive identifications (the list of these proteins is shown in Table S2). After subtracting these false positive identifications, 54 proteins remained in the FLAG-His-EWS-Fli-1 data set (shown in Table S3), including known EWS-Fli-1 interactors such as EWS (Figure 1B; Note that two EWS C-terminal peptides, which are absent in EWS-Fli-1, were identified)[8] and RNA helicase A (Figure 1C).[9] While the tandem affinity purification approach identified known interactors for EWS-Fli-1, we noticed that the majority of FLAG-His-EWS-Fli-1 expressed in 293T cells was not solubilized under the non-denaturing solubilization conditions used for tandem affinity purification (Figure 1D).

Therefore, as an alternative approach to dissect the EWS-Fli-1 interactome, we used the proximity-dependent biotinylation technique, BioID.[10] In the BioID approach, a bait protein is fused to a mutated BirA biotinylase (BirA R118G) which promiscuously biotinylates the lysine residues of proteins in the vicinity (within 20−30 nm). The biotinylated vicinal proteins are purified by streptavidin affinity chromatography and are identified by mass spectrometry. The BioID approach does not require the purification of a stable protein complex under non-denaturing conditions and is useful for the analysis of insoluble protein complexes or transient low-affinity interactions. It has been successfully applied to identify interactors for nuclear lamin A,[10] whose insolubility has hampered the analysis of its interactors, and to identify the protein components of bilobe,[17] an insoluble cytoskeletal structure in *Trypanosoma brucei*.

We expressed BioID-tagged EWS-Fli-1 in human embryonic kidney 293 cells, induced the biotinylation of the proteins in the vicinity of BioID-EWS-Fli-1 by 50 $\mu$M biotin, and isolated the biotinylated proteins by streptavidin affinity chromatography (Figure 2A). The biotinylated proteins were analyzed as described in the Experimental Procedures. At a Protein Prophet


dx.doi.org/10.1021/pr500387m | *J. Proteome Res.* 2014, 13, 3783−3791

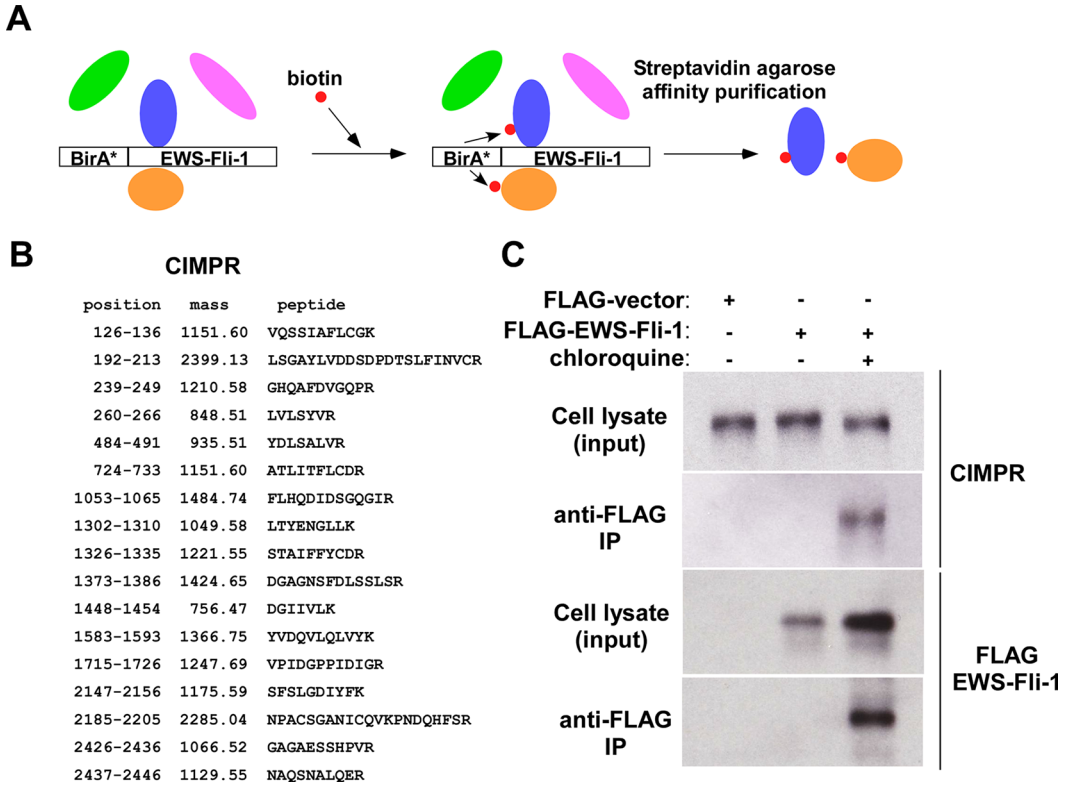


**Figure 2.** Proximity-dependent biotinylation analysis using BioID-EWS-Fli-1. (A) Proximity-dependent biotinylation procedure. 293 cells were transfected with BioID-EWS-Fli-1 (Myc tag and BirA R118G mutant fused to EWS-Fli-1), and the biotinylation of proteins in the vicinity of BioID-EWS-Fli-1 was induced by the addition of 50 $\mu$M biotin to the culture medium. The biotinylated vicinal proteins were purified by streptavidin agarose chromatography and were analyzed by tandem mass spectrometry. (B) CIMPR peptides assigned with high confidence. (C) Co-immunoprecipitation of EWS-Fli-1 and CIMPR. 293T cells were transfected with FLAG-EWS-Fli-1 or FLAG-vector. The transfected cells were treated with 100 $\mu$M chloroquine for 12 h where indicated. The physical interaction of FLAG-EWS-Fli-1 and CIMPR was examined by anti-FLAG immunoprecipitation followed by anti-CIMPR immunoblotting. The immunoprecipitation of FLAG-EWS-Fli-1 was verified by anti-FLAG immunoblotting.

probability score of 0.9 or higher, 561 different proteins were identified (Table S4). To exclude the false positive identifications, we employed the CRAPome database,[18] which is a "contaminant repository for affinity purification". Using CRAPome version 1.1 (http://www.crapome.org/), 12 control proximity-dependent biotinylation experiments performed in 293 cells were compiled. The proteins detected with five or more spectral counts per control experiment were considered as false positive identifications by the proximity-dependent biotinylation approach. The list of these false positive identifications is shown in Table S5, which contains 656 proteins. After subtracting these false positive identifications from Table S4, 366 proteins remained (Table S6), including EWS, which was shown to form a hetero-oligomer with EWS-Fli-1.[8]

After excluding the false positive identifications, 54 proteins were identified from FLAG-His-EWS-Fli-1 affinity purification and 366 proteins were identified from BioID-EWS-Fli-1 analysis, and of these, four proteins were in common: EWS-Fli-1, HNRNPA3, U2AF1, and EWS. Additionally, different isoforms of SUMO proteins were identified in both FLAG-His-EWS-Fli-1 and BioID-EWS-Fli-1 experiments. We note that there is a possible SUMO-binding motif (LELLSDS, residues 340−346) in EWS-Fli-1, which could mediate the interaction with SUMO proteins. EWS-Fli-1 does not contain a sumoylation motif (hydrophobic-K-X-E), and we have not been able to detect its sumoylation (data not shown).

Among the high-scoring proteins identified by the BioID approach, cation-independent mannose 6-phosphate receptor (CIMPR) caught our attention because the detection of CIMPR, which is a cargo that mediates the sorting of lysosomal hydrolase precursors from the trans-Golgi network to endosomes,[11] using BioID-EWS-Fli-1 suggested a possible new link between EWS-Fli-1 and the endosome−lysosome system. Molecular biological characterization of EWS-Fli-1, performed in parallel with the proteomic analyses, demonstrated that EWS-Fli-1 is a relatively stable protein and does not turn over by a proteasome-dependent mechanism (described below), which led us to consider a possibility that EWS-Fli-1 turns over by a lysosome-dependent mechanism.

In the BioID-EWS-Fli-1 experiment, 17 unique and 19 total peptides from CIMPR were identified (Figure 2B and Table S6). Consistent with the identification of CIMPR by the BioID approach, we observed the coimmunoprecipitation of FLAG-EWS-Fli-1 and endogenous CIMPR upon treatment with chloroquine, an inhibitor of lysosomal degradation (Figure 2C). It is noteworthy that CIMPR was identified by the BioID approach using only three 15-cm plates of cells whereas it was not identified by the tandem affinity purification approach using 40 15-cm plates of cells (even though the latter used 293T cells which generally result in higher protein expression levels than 293 cells employed in the former). We believe this is related to the insolubility of EWS-Fli-1 under the solubilization conditions used for tandem affinity purification (Figure 1D).


dx.doi.org/10.1021/pr500387m | J. Proteome Res. 2014, 13, 3783−3791

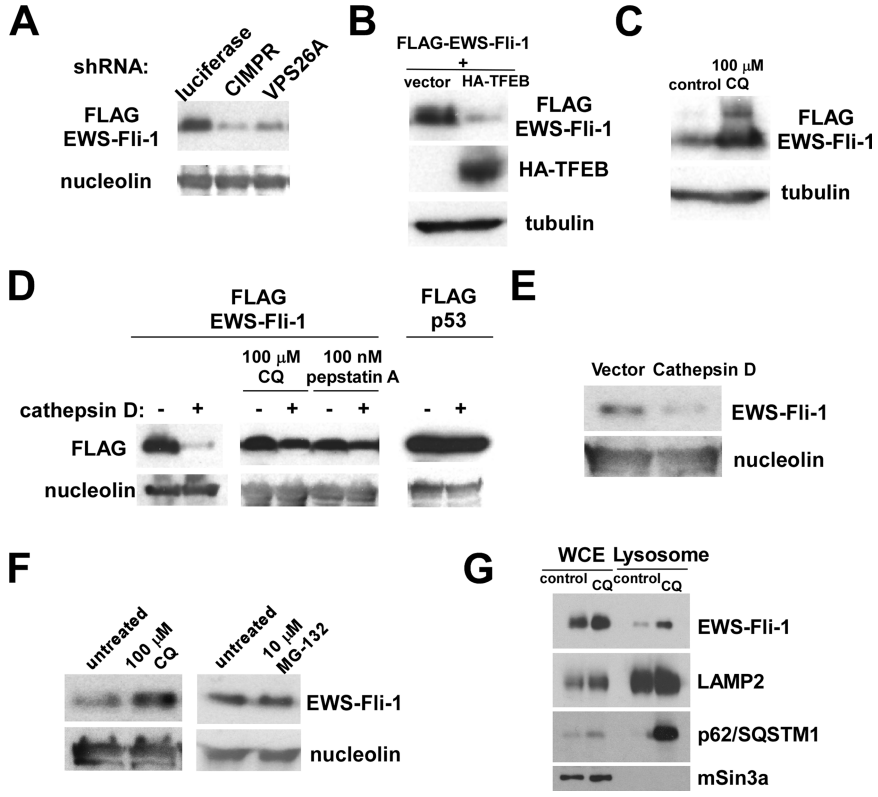


**Figure 3.** EWS-Fli-1 turns over by a lysosome-dependent mechanism: (A) Knockdown of CIMPR or VPS26A results in destabilization of FLAG-EWS-Fli-1. 293 cells were cotransfected with FLAG-EWS-Fli-1 and shRNA against luciferase (control), CIMPR, or VPS26A. Forty-eight hours after transfection, the levels of FLAG-EWS-Fli-1 were examined by anti-FLAG immunoblotting. Nucleolin serves as a loading control. (B) TFEB induces EWS-Fli-1 degradation in 293 cells. 293 cells were cotransfected with FLAG-EWS-Fli-1 and HA-TFEB or empty vector. Forty-eight hours after transfection, the levels of FLAG-EWS-Fli-1 were examined by anti-FLAG immunoblotting. Tubulin serves as a loading control. (C) Chloroquine stabilizes EWS-Fli-1 in 293 cells. 293 cells were transfected with FLAG-EWS-Fli-1. Transfected cells were left untreated (control) or treated with 100 $\mu$M chloroquine for 12 h. The levels of FLAG-EWS-Fli-1 were examined by anti-FLAG immunoblotting. Tubulin serves as a loading control. (D) Cathepsin D degrades EWS-Fli-1, but not p53, in 293 cells. 293 cells were cotransfected with FLAG-EWS-Fli-1 and cathepsin D or empty vector. Transfected cells were left untreated or treated with 100 $\mu$M chloroquine for 12 h or 100 nM pepstatin A for 12 h. 293 cells were cotransfected with FLAG-p53 and cathepsin D or empty vector. The levels of FLAG-EWS-Fli-1 and FLAG-p53 were examined by anti-FLAG immunoblotting. Nucleolin serves as a loading control. (E) Cathepsin D degrades endogenous EWS-Fli-1 in A673 Ewing sarcoma cells. A673 cells were infected with a lentivirus vector expressing cathepsin D or an empty vector, the infected cells were selected with puromycin, and the levels of endogenous EWS-Fli-1 were examined by anti-Fli-1 C-terminus antibody immunoblotting at 4 days after infection. Nucleolin serves as a loading control. (F) Chloroquine stabilizes endogenous EWS-Fli-1 in A673 cells. A673 cells were left untreated, treated with 100 $\mu$M chloroquine for 12 h, or treated with 10 $\mu$M MG-132 for 12 h. The levels of EWS-Fli-1 were examined by anti-Fli-1 C-terminus immunoblotting. While chloroquine increased the levels of endogenous EWS-Fli-1, MG-132 had no effect on the EWS-Fli-1 protein levels, suggesting that EWS-Fli-1 turns over by a lysosomal, but not proteasomal mechanism. (G) Endogenous EWS-Fli-1 in A673 cells displays increased lysosomal location upon chloroquine treatment. A673 cells were treated with 100 $\mu$M chloroquine for 12 h or left untreated, and the whole cell extract (WCE) and lysosomal fraction were isolated. The abundance of EWS-Fli-1, LAMP2, p62/SQSTM1, and mSin3A in each fraction was determined by immunoblotting.

348 peptides derived from EWS-Fli-1 were identified by the BioID approach using three 15-cm plates (Table S6) whereas 120 peptides derived from EWS-Fli-1 were identified by the tandem affinity purification approach using 40 15-cm plates (Table S3), suggesting the efficient solubilization of EWS-Fli-1 by the BioID lysis buffer which contains 0.4% SDS. Our result as well as two previous BioID studies[10,17] suggest the utility of the BioID approach for the dissection of protein−protein interactions involving insoluble proteins.

## EWS-Fli-1 Turnover Occurs via a Lysosome-Dependent Mechanism

The protein transport function of CIMPR is regulated by the retromer complex, which redirects CIMPR from the endosome to the trans-Golgi network.[19,20] Interestingly, knockdown of CIMPR or VPS26A, an essential component of the retromer, resulted in reduced EWS-Fli-1 protein expression (Figure 3A). This raised a possibility that EWS-Fli-1 is transported to the late endosome and degraded by the lysosome, especially when CIMPR and retromer functions are compromised. Importantly, we found that coexpression of TFEB, a potent inducer of lysosomal biogenesis,[21] resulted in striking degradation of EWS-Fli-1 (Figure 3B). Conversely, inhibition of lysosomal degradation by chloroquine stabilized EWS-Fli-1 (Figure 3C). Lysosomes contain many hydrolases that degrade various biomolecules, including proteins. We found that one of the lysosomal proteases, cathepsin D, can degrade EWS-Fli-1, which was inhibited by chloroquine or a cathepsin D inhibitor, pepstatin A (Figure 3D). Cathepsin D did not degrade p53 (Figure 3D), indicating that cathepsin D does not degrade proteins non-selectively. Furthermore, we found that endogenous EWS-Fli-1 in A673 Ewing sarcoma cells is degraded upon expression of cathepsin D (Figure 3E) and is stabilized by chloroquine, an inhibitor of lysosomal degradation (Figure 3F,


dx.doi.org/10.1021/pr500387m | J. Proteome Res. 2014, 13, 3783−3791

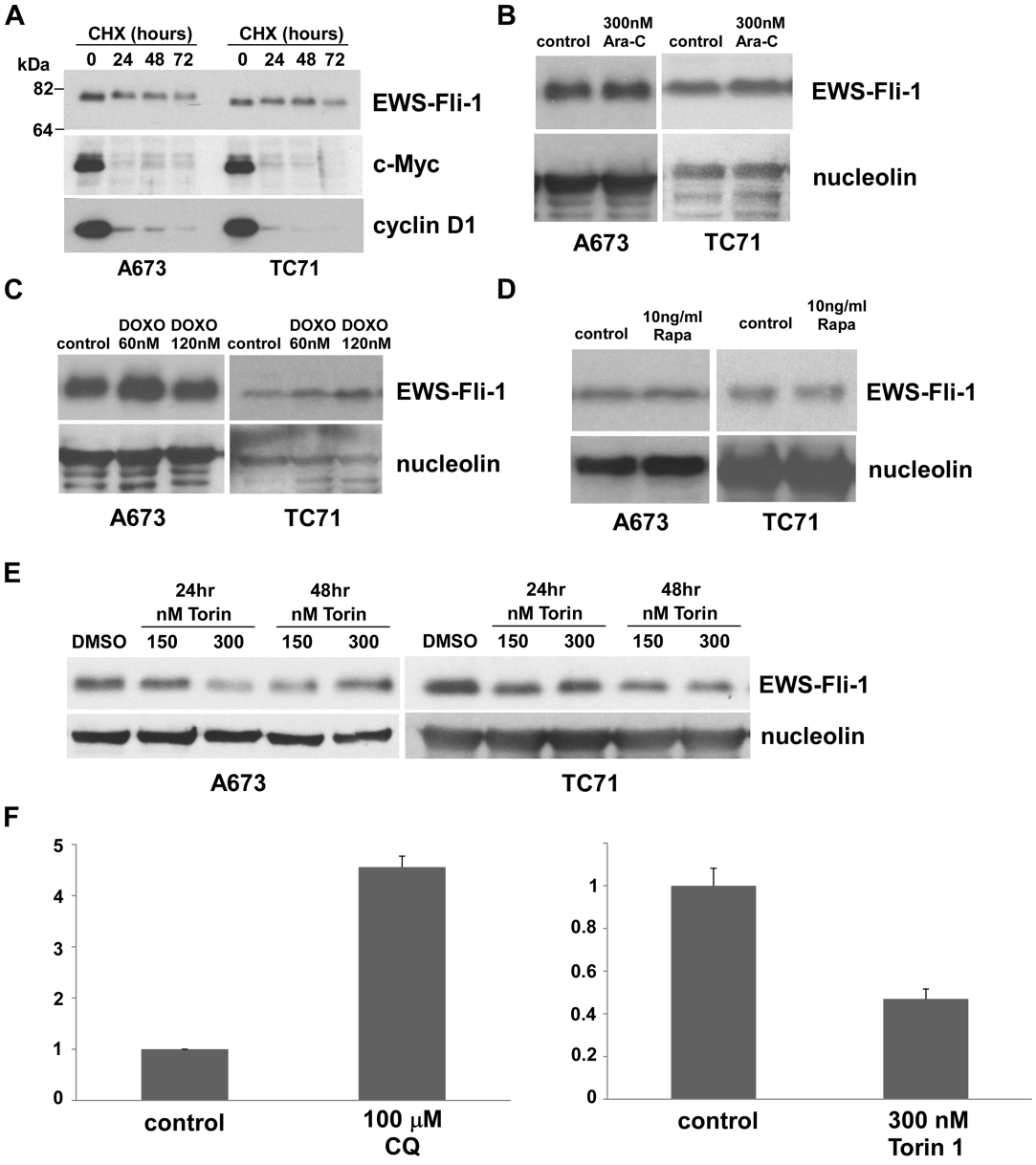


**Figure 4.** Targeting EWS-Fli-1 for degradation: (A) The effects of cycloheximide on endogenous EWS-Fli-1 levels in Ewing sarcoma cells. To reduce the toxicity of cycloheximide, ubiquitin was exogenously expressed in A673 and TC71 cells. Subsequently, A673 and TC71 cells were treated with 100 $\mu$g/mL cycloheximide for 24, 48, or 72 h and the levels of EWS-Fli-1, c-Myc, and cyclin D1 were determined by anti-Fli-1 C-terminus, anti-c-Myc, and anti-cyclin D1 immunoblotting, respectively. Thirty $\mu$g of whole cell lysate was loaded in each lane. (B) The effects of cytosine arabinoside on endogenous EWS-Fli-1 levels in Ewing sarcoma cells. A673 and TC71 cells were treated with 300 nM cytosine arabinoside for 48 h, and the levels of endogenous EWS-Fli-1 were determined by anti-Fli-1 C-terminus immunoblotting. Nucleolin serves as a loading control. (C) The effects of doxorubicin on endogenous EWS-Fli-1 levels in Ewing sarcoma cells. A673 and TC71 cells were treated with 60 or 120 nM doxorubicin for 72 h, and the levels of endogenous EWS-Fli-1 were determined by anti-Fli-1 C-terminus immunoblotting. Nucleolin serves as a loading control. (D) The effects of rapamycin on endogenous EWS-Fli-1 levels in Ewing sarcoma cells. A673 and TC71 cells were treated with 10 ng/mL rapamycin for 48 h, and the levels of endogenous EWS-Fli-1 were determined by anti-Fli-1 C-terminus immunoblotting. Nucleolin serves as a loading control. (E) Torin 1 reduces the EWS-Fli-1 protein levels in Ewing sarcoma. A673 and TC71 cells were left untreated or treated with 150 or 300 nM torin 1 for 24 or 48 h. The levels of endogenous EWS-Fli-1 were determined by anti-Fli-1 C-terminus immunoblotting. The experiment was repeated three times with similar results. Nucleolin serves as a loading control. (F) Luminescent monitoring of EWS-Fli-1 protein levels. 293 cells were infected with a lentivirus vector expressing luciferase−EWS-Fli-1 fusion protein, and the infected cells were selected with puromycin. The cells were treated with 100 $\mu$M chloroquine for 12 h or left untreated, and the luciferase activity was determined using the same amount of protein lysate (left). The cells were treated with 300 nM torin 1 for 24 h or left untreated, and the luciferase activity was determined using the same amount of protein lysate (right).

left). Endogenous EWS-Fli-1 in A673 cells was not stabilized by a proteasome inhibitor, MG-132 (Figure 3F, right). Using subcellular fractionation, we detected endogenous EWS-Fli-1 in the lysosomal fraction, which increased upon chloroquine treatment (Figure 3G). An abundant lysosomal glycoprotein, LAMP2, was readily detectable in the lysosomal fraction whereas a nuclear transcriptional corepressor mSin3A, which is not known to be located in the lysosome, was absent (Figure 3G). p62/SQSTM1, a known substrate of lysosomal degradation, displayed increased lysosomal location upon chloroquine


dx.doi.org/10.1021/pr500387m | J. Proteome Res. 2014, 13, 3783−3791

treatment (Figure 3G). These results indicate that EWS-Fli-1 is degraded by the lysosome.

### Targeting EWS-Fli-1 for Degradation

We employed a translational inhibitor, cycloheximide, to inhibit the new protein synthesis in Ewing sarcoma cells and analyzed the turnover of endogenous EWS-Fli-1 protein. While the EWS-Fli-1 protein levels did not exhibit any significant decrease after 24 h treatment with cycloheximide, the sensitivity of Ewing sarcoma cells to cycloheximide did not allow us to continue the cycloheximide treatment to observe the turnover of EWS-Fli-1, which is consistent with a previous report.[22] The toxicity of translation inhibitors such as cycloheximide was attributed to the depletion of ubiquitin.[23] Therefore, we exogenously expressed ubiquitin in Ewing sarcoma cells, which made the cells less sensitive to cycloheximide, and analyzed EWS-Fli-1 turnover upon prolonged cycloheximide treatment. We observed some decay of EWS-Fli-1 after 72 h treatment with cycloheximide (Figure 4A). In contrast, c-Myc [half-life = ∼30 min[24]] and cyclin D1 [half-life <30 min[25]] displayed the expected rapid decay upon cycloheximide treatment (Figure 4A). Our data suggest that endogenous EWS-Fli-1 is a relatively stable protein, which agrees with the previous findings on transfected EWS-Fli-1[26] and Fli-1.[27]

Since EWS-Fli-1 is a stable protein, there is a large therapeutic window to enhance its degradation. There are a few previously reported compounds that reduce EWS-Fli-1 protein levels. Rapamycin, an mTOR allosteric inhibitor, was reported to diminish EWS-Fli-1 protein levels in several Ewing sarcoma cell lines.[28] A screening for chemical compounds that inhibit the EWS-Fli-1-mediated gene expression signature identified cytosine arabinoside, which was later shown to reduce the EWS-Fli-1 protein levels in Ewing sarcoma cells.[29] The same study also demonstrated that doxorubicin, one of the standard chemotherapeutic agents for treating Ewing sarcoma, can reduce EWS-Fli-1 protein levels in Ewing sarcoma cells. However, using the conditions described in refs 28 and 29, we have been unable to reproduce the reported effects of cytosine arabinoside, doxorubicin, and rapamycin on EWS-Fli-1 protein levels (Figure 4B–D).

A transcription factor TFEB recently emerged as a master regulator of lysosomal biogenesis.[21] The activity of TFEB is controlled by cytoplasmic sequestration, which is regulated by mTOR-mediated phosphorylation.[30−32] A potent mTOR active-site inhibitor, torin 1, was shown to efficiently induce the nuclear translocation of TFEB.[30−32] In contrast, rapamycin, an mTOR allosteric inhibitor that only incompletely inhibits mTOR activity, did not induce TFEB nuclear translocation at any of the concentrations that are routinely used (10 nM − 10 $\mu$M).[30,31] We found that torin 1 treatment of Ewing sarcoma cells resulted in reduced EWS-Fli-1 protein levels (Figure 4E), suggesting a potential therapeutic utility of mTOR active-site inhibitors against Ewing sarcoma.

We also devised the fusion of EWS-Fli-1 and firefly luciferase to monitor the EWS-Fli-1 protein levels. The luciferase activity derived from the luciferase−EWS-Fli-1 fusion protein increased upon chloroquine treatment and decreased by torin 1 treatment (Figure 4F), further supporting that EWS-Fli-1 turns over by a lysosome-dependent mechanism, which can be enhanced by torin 1. In addition, this luciferase reporter can be used in the future to screen for compounds that target EWS-Fli-1 for degradation.

Since the discovery of chromosomal translocation generating the EWS-Fli-1 fusion oncogene and the pivotal role played by the transcriptional activity of EWS-Fli-1 in Ewing sarcoma, several attempts have been made to target the transcriptional activity of EWS-Fli-1. Stegmaier et al. screened a small molecule library for compounds that inhibit the gene expression signature mediated by EWS-Fli-1 in A673 Ewing sarcoma cells and identified cytosine arabinoside as an EWS-Fli-1 modulator.[29] Erkizan et al. employed surface plasmon resonance screening for compounds that bind EWS-Fli-1 and identified a small molecule that blocks the interaction of EWS-Fli-1 and RNA helicase A, leading to suppression of EWS-Fli-1 transcriptional activity and Ewing sarcoma growth.[33] Grohar et al. employed a high throughput screen (luciferase reporter screen followed by a gene signature secondary screen) to evaluate over 50,000 compounds for inhibition of EWS-Fli-1 transcriptional activity and identified mithramycin as an EWS-Fli-1 inhibitor displaying anti-Ewing sarcoma activity.[34] Boro et al. used four EWS-Fli-1 transcriptional target genes as readout to screen for compounds that abrogate EWS-Fli-1 transcriptional activity and identified a kinase inhibitor, midostaurin, which induced apoptosis in Ewing sarcoma cells.[35] While these seminal attempts provided important insights into Ewing sarcoma biology, an EWS-Fli-1-targeted therapy has not reached clinical translation and EWS-Fli-1 remains "the perfect target without a therapeutic agent".[7] Our findings that EWS-Fli-1 turns over by a lysosome-dependent mechanism and that an mTORC1 active-site inhibitor can reduce the EWS-Fli-1 protein levels in Ewing sarcoma cells suggest a potential therapy by targeting EWS-Fli-1 for degradation.

## CONCLUSIONS

Proteomic analysis of the EWS-Fli-1 interactome led to the discovery of the role for the lysosome in EWS-Fli-1 protein turnover. We demonstrated that EWS-Fli-1 is a stable protein, which provides a large therapeutic window to enhance its degradation. We found that an mTORC1 active-site inhibitor, torin 1, which stimulates the TFEB-lysosome pathway, can induce the degradation of EWS-Fli-1 in Ewing sarcoma cells. mTORC1 active-site inhibitors could target both the dependence of Ewing sarcoma on IGF-mTOR signaling and EWS-Fli-1 protein turnover and are potentially more effective than mTOR allosteric inhibitors as therapy for Ewing sarcoma.

## ASSOCIATED CONTENT

### Supporting Information

Table S1: Preliminary list of FLAG-His-EWS-Fli-1 interacting proteins. Table S2: List of proteins commonly identified by FLAG-His-EWS-Fli-1 and FLAG-His-p21 or FLAG-His-macro-H2A. Table S3: List of FLAG-His-EWS-Fli-1 interacting proteins after exclusion of proteins in Table S2. Table S4: Preliminary list of proteins identified by proximity-dependent biotinylation using BioID-EWS-Fli-1. Table S5: List of false positive identifications by proximity-dependent biotinylation derived from the CRAPome database. Table S6: List of proteins identified by proximity-dependent biotinylation using BioID-EWS-Fli-1 after exclusion of proteins in Table S5. Tables S1 and S4 list the proteins identified with a Protein Prophet probability score of 0.9 or higher, which corresponded to false identification rates of 1.1% and 0.7% in FLAG-His-EWS-Fli-1 and BioID-EWS-Fli-1 data sets, respectively. This material is available free of charge via the Internet at http://pubs.acs.org.

## AUTHOR INFORMATION

### Corresponding Author

*Tel: +1-210-562-9089; Fax: +1-210-562-9014; E-mail shiio@uthscsa.edu.

### Notes

The authors declare no competing financial interest.

## ACKNOWLEDGMENTS

We thank Mr. Barron Blackman for assistance with proteomics informatics. This work was supported by the Owens Medical Research Foundation Grant #154005, Department of Defense Grant W81 XWH-13-1-0280, NIH Grant UL1TR001120 from the National Center for Advancing Translational Sciences (to Y.S.), NIH shared instrumentation Grant S10RR025111 (to S.T.W.), and NIH Grant CA054174 (Cancer Therapy and Research Center at UTHSCSA—Mass Spectrometry Shared Resource).

## REFERENCES

(1) Toomey, E. C.; Schiffman, J. D.; Lessnick, S. L. Recent advances in the molecular pathogenesis of Ewing's sarcoma. *Oncogene* **2010**, *29* (32), 4504−16.

(2) Mackintosh, C.; Madoz-Gurpide, J.; Ordonez, J. L.; Osuna, D.; Herrero-Martin, D. The molecular pathogenesis of Ewing's sarcoma. *Cancer Biol. Ther.* **2010**, *9* (9), 655−67.

(3) Jedlicka, P. Ewing Sarcoma, an enigmatic malignancy of likely progenitor cell origin, driven by transcription factor oncogenic fusions. *Int. J. Clin. Exp. Pathol.* **2010**, *3* (4), 338−47.

(4) Lessnick, S. L.; Ladanyi, M. Molecular pathogenesis of Ewing sarcoma: new therapeutic and transcriptional targets. *Annu. Rev. Pathol.* **2012**, *7*, 145−59.

(5) Grohar, P. J.; Helman, L. J. Prospects and challenges for the development of new therapies for Ewing sarcoma. *Pharmacol. Ther.* **2012**, *137* (2), 216−24.

(6) Prieur, A.; Tirode, F.; Cohen, P.; Delattre, O. EWS/FLI-1 silencing and gene profiling of Ewing cells reveal downstream oncogenic pathways and a crucial role for repression of insulin-like growth factor binding protein 3. *Mol. Cell. Biol.* **2004**, *24* (16), 7275−83.

(7) Uren, A.; Toretsky, J. A. Ewing's sarcoma oncoprotein EWS-FLI1: the perfect target without a therapeutic agent. *Future Oncol.* **2005**, *1* (4), 521−8.

(8) Spahn, L.; Siligan, C.; Bachmaier, R.; Schmid, J. A.; Aryee, D. N.; Kovar, H. Homotypic and heterotypic interactions of EWS, FLI1 and their oncogenic fusion protein. *Oncogene* **2003**, *22* (44), 6819−29.

(9) Toretsky, J. A.; Erkizan, V.; Levenson, A.; Abaan, O. D.; Parvin, J. D.; Cripe, T. P.; Rice, A. M.; Lee, S. B.; Uren, A. Oncoprotein EWS-FLI1 activity is enhanced by RNA helicase A. *Cancer Res.* **2006**, *66* (11), 5574−81.

(10) Roux, K. J.; Kim, D. I.; Raida, M.; Burke, B. A promiscuous biotin ligase fusion protein identifies proximal and interacting proteins in mammalian cells. *J. Cell Biol.* **2012**, *196* (6), 801−10.

(11) Ghosh, P.; Dahms, N. M.; Kornfeld, S. Mannose 6-phosphate receptors: new twists in the tale. *Nat. Rev. Mol. Cell Biol.* **2003**, *4* (3), 202−12.

(12) Elzi, D. J.; Lai, Y.; Song, M.; Hakala, K.; Weintraub, S. T.; Shiio, Y. Plasminogen activator inhibitor 1—insulin-like growth factor binding protein 3 cascade regulates stress-induced senescence. *Proc. Natl. Acad. Sci. U. S. A.* **2012**, *109* (30), 12052−7.

(13) Elzi, D. J.; Song, M.; Hakala, K.; Weintraub, S. T.; Shiio, Y. Wnt Antagonist SFRP1 Functions as a Secreted Mediator of Senescence. *Mol. Cell. Biol.* **2012**, *32* (21), 4388−99.

(14) Deutsch, E. W.; Mendoza, L.; Shteynberg, D.; Farrah, T.; Lam, H.; Tasman, N.; Sun, Z.; Nilsson, E.; Pratt, B.; Prazen, B.; Eng, J. K.; Martin, D. B.; Nesvizhskii, A. I.; Aebersold, R. A guided tour of the Trans-Proteomic Pipeline. *Proteomics* **2010**, *10* (6), 1150−9.

(15) Keller, A.; Nesvizhskii, A. I.; Kolker, E.; Aebersold, R. Empirical statistical model to estimate the accuracy of peptide identifications made by MS/MS and database search. *Anal. Chem.* **2002**, *74* (20), 5383−92.

(16) Nesvizhskii, A. I.; Keller, A.; Kolker, E.; Aebersold, R. A statistical model for identifying proteins by tandem mass spectrometry. *Anal. Chem.* **2003**, *75* (17), 4646−58.

(17) Morriswood, B.; Havlicek, K.; Demmel, L.; Yavuz, S.; Sealey-Cardona, M.; Vidilaseris, K.; Anrather, D.; Kostan, J.; Djinovic-Carugo, K.; Roux, K.; Warren, G. Novel bilobe components in Trypanosoma brucei identified using proximity-dependent biotinylation. *Eukaryote Cell* **2013**, *12*, 356.

(18) Mellacheruvu, D.; Wright, Z.; Couzens, A. L.; Lambert, J. P.; St-Denis, N. A.; Li, T.; Miteva, Y. V.; Hauri, S.; Sardiu, M. E.; Low, T. Y.; Halim, V. A.; Bagshaw, R. D.; Hubner, N. C.; Al-Hakim, A.; Bouchard, A.; Faubert, D.; Fermin, D.; Dunham, W. H.; Goudreault, M.; Lin, Z. Y.; Badillo, B. G.; Pawson, T.; Durocher, D.; Coulombe, B.; Aebersold, R.; Superti-Furga, G.; Colinge, J.; Heck, A. J.; Choi, H.; Gstaiger, M.; Mohammed, S.; Cristea, I. M.; Bennett, K. L.; Washburn, M. P.; Raught, B.; Ewing, R. M.; Gingras, A. C.; Nesvizhskii, A. I. The CRAPome: a contaminant repository for affinity purification-mass spectrometry data. *Nat. Methods* **2013**, *10* (8), 730−6.

(19) Bonifacino, J. S.; Hurley, J. H. Retromer. *Curr. Opin. Cell Biol.* **2008**, *20* (4), 427−36.

(20) Seaman, M. N. The retromer complex—endosomal protein recycling and beyond. *J. Cell Sci.* **2012**, *125* (Pt 20), 4693−702.

(21) Sardiello, M.; Palmieri, M.; di Ronza, A.; Medina, D. L.; Valenza, M.; Gennarino, V. A.; Di Malta, C.; Donaudy, F.; Embrione, V.; Polishchuk, R. S.; Banfi, S.; Parenti, G.; Cattaneo, E.; Ballabio, A. A gene network regulating lysosomal biogenesis and function. *Science* **2009**, *325* (5939), 473−7.

(22) Schlottmann, S.; Erkizan, H. V.; Barber-Rotenberg, J. S.; Knights, C.; Cheema, A.; Uren, A.; Avantaggiati, M. L.; Toretsky, J. A. Acetylation Increases EWS-FLI1 DNA Binding and Transcriptional Activity. *Front. Oncol.* **2012**, *2*, 107.

(23) Hanna, J.; Leggett, D. S.; Finley, D. Ubiquitin depletion as a key mediator of toxicity by translational inhibitors. *Mol. Cell. Biol.* **2003**, *23* (24), 9251−61.

(24) Ramsay, G.; Evan, G. I.; Bishop, J. M. The protein encoded by the human proto-oncogene c-myc. *Proc. Natl. Acad. Sci. U. S. A.* **1984**, *81* (24), 7742−6.

(25) Diehl, J. A.; Zindy, F.; Sherr, C. J. Inhibition of cyclin D1 phosphorylation on threonine-286 prevents its rapid degradation via the ubiquitin-proteasome pathway. *Genes Dev.* **1997**, *11* (8), 957−72.

(26) Bailly, R. A.; Bosselut, R.; Zucman, J.; Cormier, F.; Delattre, O.; Roussel, M.; Thomas, G.; Ghysdael, J. DNA-binding and transcriptional activation properties of the EWS-FLI-1 fusion protein resulting from the t(11;22) translocation in Ewing sarcoma. *Mol. Cell. Biol.* **1994**, *14* (5), 3230−41.

(27) Asano, Y.; Czuwara, J.; Trojanowska, M. Transforming growth factor-beta regulates DNA binding activity of transcription factor Fli1 by p300/CREB-binding protein-associated factor-dependent acetylation. *J. Biol. Chem.* **2007**, *282* (48), 34672−83.

(28) Mateo-Lozano, S.; Tirado, O. M.; Notario, V. Rapamycin induces the fusion-type independent downregulation of the EWS/FLI-1 proteins and inhibits Ewing's sarcoma cell proliferation. *Oncogene* **2003**, *22* (58), 9282−7.

(29) Stegmaier, K.; Wong, J. S.; Ross, K. N.; Chow, K. T.; Peck, D.; Wright, R. D.; Lessnick, S. L.; Kung, A. L.; Golub, T. R. Signature-based small molecule screening identifies cytosine arabinoside as an EWS/FLI modulator in Ewing sarcoma. *PLoS Med.* **2007**, *4* (4), e122.

(30) Settembre, C.; Zoncu, R.; Medina, D. L.; Vetrini, F.; Erdin, S.; Erdin, S.; Huynh, T.; Ferron, M.; Karsenty, G.; Vellard, M. C.; Facchinetti, V.; Sabatini, D. M.; Ballabio, A. A lysosome-to-nucleus signalling mechanism senses and regulates the lysosome via mTOR and TFEB. *EMBO J.* **2012**, *31* (5), 1095−108.

(31) Roczniak-Ferguson, A.; Petit, C. S.; Froehlich, F.; Qian, S.; Ky, J.; Angarola, B.; Walther, T. C.; Ferguson, S. M. The transcription

factor TFEB links mTORC1 signaling to transcriptional control of lysosome homeostasis. *Sci. Signal* **2012**, *5* (228), ra42.
(32) Martina, J. A.; Chen, Y.; Gucek, M.; Puertollano, R. MTORC1 functions as a transcriptional regulator of autophagy by preventing nuclear transport of TFEB. *Autophagy* **2012**, *8* (6), 903−14.
(33) Erkizan, H. V.; Kong, Y.; Merchant, M.; Schlottmann, S.; Barber-Rotenberg, J. S.; Yuan, L.; Abaan, O. D.; Chou, T. H.; Dakshanamurthy, S.; Brown, M. L.; Uren, A.; Toretsky, J. A. A small molecule blocking oncogenic protein EWS-FLI1 interaction with RNA helicase A inhibits growth of Ewing's sarcoma. *Nat. Med.* **2009**, *15* (7), 750−6.
(34) Grohar, P. J.; Woldemichael, G. M.; Griffin, L. B.; Mendoza, A.; Chen, Q. R.; Yeung, C.; Currier, D. G.; Davis, S.; Khanna, C.; Khan, J.; McMahon, J. B.; Helman, L. J. Identification of an inhibitor of the EWS-FLI1 oncogenic transcription factor by high-throughput screening. *J. Natl. Cancer Inst.* **2011**, *103* (12), 962−78.
(35) Boro, A.; Pretre, K.; Rechfeld, F.; Thalhammer, V.; Oesch, S.; Wachtel, M.; Schafer, B. W.; Niggli, F. K. Small-molecule screen identifies modulators of EWS/FLI1 target gene expression and cell survival in Ewing's sarcoma. *Int. J. Cancer* **2012**, *131* (9), 2153−64.